*Quantum Electronics* **50** (4) 331 – 334 (2020) 

https://doi.org/10.1070/QEL17282

# Two-stage nonlinear compression of high-power femtosecond laser pulses

V.N. Ginzburg, I.V. Yakovlev, A.S. Zuev, A.P. Korobeynikova, A.A. Kochetkov, A.A. Kuzmin, S.Yu. Mironov, A.A. Shaykin, I.A. Shaikin, E.A. Khazanov

***Abstract.*** **Two-stage compression of laser pulses with a power of 250 TW is experimentally realised by broadening their spectrum during self-phase modulation in fused silica and subsequent dispersion compensation upon reflection from chirping mirrors. A five-fold decrease in the duration is demonstrated, from 75 to 15 fs, with a *B*-integral value of about 5 at each stage. It is possible to avoid small-scale self-focusing due to self-filtering of the laser beam during free propagation in vacuum. With optimal parameters of the dispersive mirror, the pulse can be compressed to a duration of less than 5 fs.**

***Keywords:*** *high-power femtosecond laser pulses, two-stage nonlinear compression, self-phase modulation.*

## 1. Introduction

At present, the size and breakdown threshold of compressor diffraction gratings restrict the power and, therefore, the focal intensity of laser radiation. Further advancement of the technology for manufacturing gratings does not lead to qualitative improvements. A multiple increase in power is possible using mosaic gratings in the compressor (consisting of $N$ precision aligned single gratings) or creating $N$ parallel chirped pulse amplification (CPA) channels, each of which ends with a conventional compressor. In these cases, the pulse energy increases by $N$ times and, with its duration being the same, the power also increases by $N$ times. This method for increasing the pulse power entails a number of problems, namely, the complexity and dimensions of the setup, as well as its price, increase. An alternative approach developing in recent years is free from these shortcomings. In this approach the power increases not due to an increase in energy, but due to a decrease in the pulse duration after the compressor: the spectrum broadens due to self-phase modulation during propagation in a Kerr nonlinearity medium, and then the pulse is compressed by chirped mirrors (CMs) (Fig. 1). This approach is called TFC (thin film compression), TPC (thin plate compression) or CafCA (compression after compressor approach).

The idea of using cubic nonlinearity to broaden the spectrum and then compress the pulse was first proposed by Fisher et al. [1] and implemented by Laubereau [2] for picosecond pulses as early as 1969. Later, already in the femtosecond range, the idea was realised in fibres [3], in gas-filled hollow waveguides [4], in multi-pass gas cells [5] and in a solid with a restriction in the transverse direction [6]. However, it was possible to achieve compression of pulses with an energy of only about millijoule, and with an efficiency of less than 50%. In the past few years, a number of experimental results have been obtained [7 – 10], in which CafCA was successfully implemented for pulses with an energy of more than 1 J, and with an efficiency close to 100%. An important motivation for these studies was provided by the proposed and experimentally confirmed method for suppressing small-scale self-focusing [11, 12], which can significantly increase the compression ratio. More details about the CafCA method can be found in review [13].

One of the advantages of this method is the ability to apply it sequentially. For example, in two-stage geometry, two sequential compressions are performed: a nonlinear element, a chirped mirror (mirrors), another nonlinear element, one more chirped mirror (mirrors) (see Fig. 1). This approach was used at a microjoule level [14 – 16]. However, in ultrahigh-power lasers at the second stage, it is necessary to use very thin nonlinear elements with a thickness of the order of ~100 μm, which is possible only when using plastic. That is why previously only fragmentation of a nonlinear element and single compression for glass were considered [17, 18], which is much less efficient than two-stage compression [13]. The idea of applying two-stage compression for ultrahigh-power pulses was proposed in the same paper in which the idea of using plastic was expressed [19] and where the possibility of compressing a pulse from 27 to 2.1 fs was theoretically shown. In this work, we report on the experimental implementation of two-stage compression, in which the pulse at the output of a laser with a power of 250 TW was compressed by five times.

## 2. Experimental results

A schematic of the experiment is shown in Fig. 1. A beam from the PEARL laser [20] (centre wavelength $\lambda = 910$ nm) with a pulse energy of up to 17 J, a duration of 60 – 75 fs, and a diameter of 18 cm, after reflection from the last diffraction grating of the compressor, propagated in a free space of 2.5 m for self-filtration [11, 21]. Next, there were three fused silica plates 1 mm thick each. We used three plates instead of one (3 mm thick) to reduce small-scale self-focusing [13]. At a distance of 4 m from them, the CMs of the first stage were installed. Then, after 2 m of free propagation, the beam passed through one silica plate with a thickness of 1 mm and

**V.N. Ginzburg, I.V. Yakovlev, A.S. Zuev, A.P. Korobeynikova, A.A. Kochetkov, A.A. Kuzmin, S.Yu. Mironov, A.A. Shaykin, I.A. Shaikin, E.A. Khazanov** Institute of Applied Physics, Russian Academy of Sciences, ul. Ulyanova 46, 603950 Nizhny Novgorod, Russia; e-mail: vlgin@rambler.ru

Received 17 January 2020
*Kvantovaya Elektronika* **50** (4) 331 – 334 (2020)
Translated by V.L. Derbov

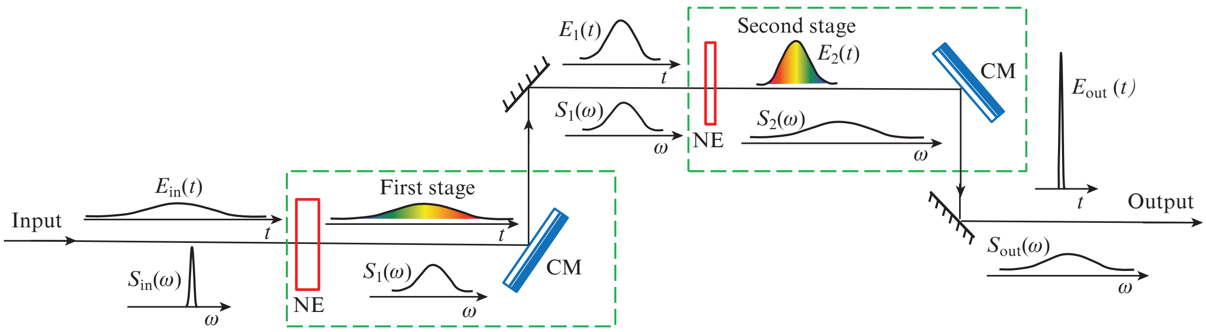


**Figure 1.** Scheme of two-stage non-linear compression: (NE) nonlinear element (silica plate); (CM) chirped mirror.

was directed to the CM of the second stage. All CMs had a dispersion of –100 fs$^2$ and a reflection coefficient of 99.5% in the band 810–1010 nm (UltraFast Innovations GmbH).

To measure the parameters of the input and output pulses, two glass wedges with an aperture of 1 × 2 cm and a frosted back surface were introduced into the beam: one was installed before the plates of the first stage, and the other, after the last CM. The beams reflected from the wedges were sent to two spectrometers and two autocorrelators. The laser beam was sufficiently uniform in cross section; the spectra and durations of the input and output pulses without silica plates coincided with an accuracy of 10%. Thus, it was possible to measure the spectra and autocorrelation functions (ACF) of the input and output pulses in one laser shot. Below, by experimentally measured pulse duration, we mean the full width at half-maximum (FWHM) of its ACF divided by $\sqrt{2}$.

We compared the single-stage and two-stage geometries in two versions: two CMs at the first stage plus two CMs in the second one and three CMs at the first stage plus one CM in the second one. In Fig. 2a, the pulse compression factor $F = \tau_{in}/\tau_{out}$ (the ratio of ACF FWHMs of the input and output pulses) is plotted versus the value of the *B*-integral at the first stage:

$$B = kLn_2I,$$

where $I$ is the input intensity; $L$ is the total thickness of the plates of the first stage; $n_2 = 3 \times 10^{-16}$ cm$^2$ W$^{-1}$ is the nonlinear refractive index; $k = 2\pi/\lambda$; and $\lambda = 910$ nm. The observed scatter of the experimental data in Fig. 2a is due to the error in the determination of the *B*-integral, as well as the instability of the spectral and temporal characteristics of the radiation.

The efficiency of the second stage is most clearly visible if the first stage uses two CMs (compare the dark and light circles in Fig. 2a). If the first stage uses three CMs, then the second stage improves compression only at $B = 5–6$. Note that this is in qualitative agreement with the theoretical curves plotted for the typical input pulse used in the experiment. Theoretical calculations of nonlinear propagation in silica were carried out in the second-order approximation of the dispersion theory. It is important to note that for a fixed plate thickness for the most optimal compression at both stages, it is necessary to use CMs with dispersion depending on the *B*-integral, and for $B > 2$ this dependence decreases monotonically: the greater the *B*-integral, the smaller (in absolute value) should be the CM dispersion [13, 22]. Thus, for large values of the *B*-integral, very small dispersion values are

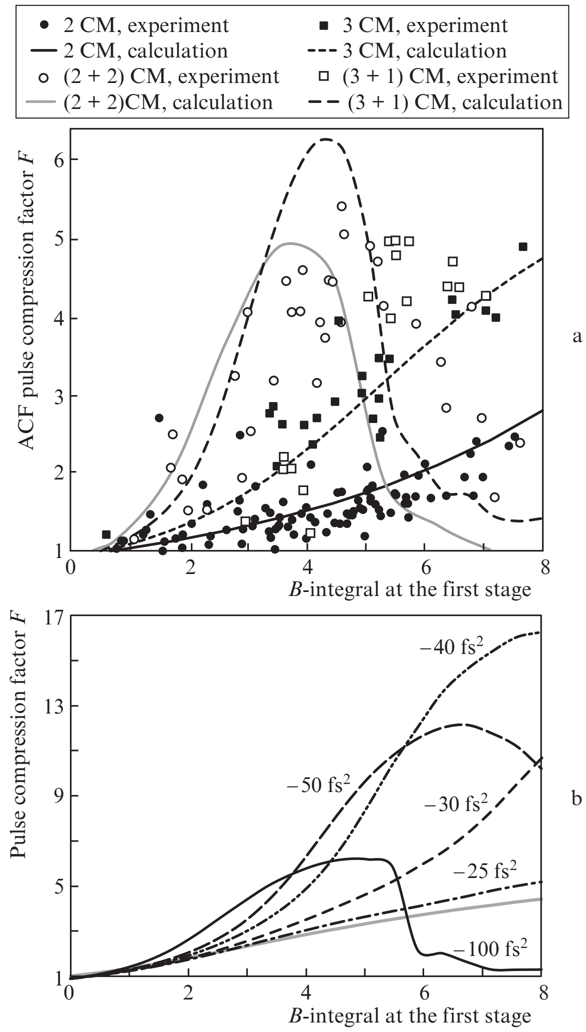


**Figure 2.** Dependence of the pulse compression factor $F = \tau_{in}/\tau_{out}$ on the value of the *B*-integral at the first stage: (a) experiment for single-stage (dark points) and two-stage (light points) geometry, as well as (b) calculation for one stage (grey curve) and different CM dispersion values at the second stage.

needed. For a given CM dispersion, the dependence of the compression ratio $F$ on the *B*-integral is nonmonotonic and has a maximum. This is clearly seen in Fig. 2a for two-stage geometry. A decrease in $F$ for large values of the *B*-integral is explained by the fact that the spectrum of the pulse at the output of the second stage becomes so broad that the excess dispersion of the CM greatly stretches the pulse. In the experiment, only mirrors with a dispersion of –100 $fs^2$ were available to us, while the optimal value for the second stage (for large *B*) should be much smaller (about –40 $fs^2$).

In Fig. 2b, the theoretical dependences of the compression factor for a pulse with the initial duration of 70 fs are plotted for different CMs at the second stage (at the first stage, the dispersion of the CM is –300 $fs^2$). It can be seen that the compression efficiency strongly depends on the CM at the second stage, and the optimal selection of the CM allows the pulse to be compressed to a duration shorter than 5 fs while compensating only for the quadratic spectral phase. We also note that taking into account the third and higher orders of material dispersion of the plates increases the pulse duration by less than 10%.

Figure 3 shows the experimental dependences of the output pulse duration on the input duration in one- and two-stage schemes for the values of the first-stage *B*-integral equal to 3–6 for two and 5–7 for three CMs at the first stage. Durations were calculated from ACFs of the pulses. Figure 3 also demonstrates well the efficiency of using the second stage: dark points are located significantly higher than light ones. In addition, it can be seen that the duration of all output pulses in the (3 + 1) CM scheme lies in the range of 14–16 fs regardless of the duration of the input pulse. A possible reason for this may be the insufficiently broad spectral band of the used CMs, as well as the instrument function of the autocorrelator.

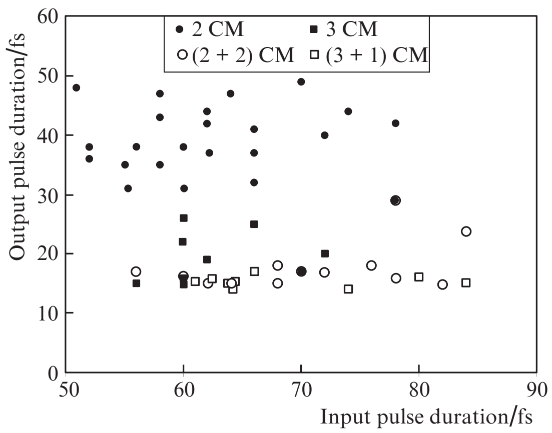


**Figure 3.** Dependences of the output pulse duration on the input pulse duration for single-stage (dark dots) and two-stage (light dots) geometry.

Figure 4 shows typical spectra and ACFs of the input and output pulses in a scheme with three CMs at the first stage and one CM at the second one. A significant broadening of the spectrum of the pulse after self-phase modulation is seen (Fig. 4a). The presence of narrow peaks in the spectrum of the output pulse is due to the fact that the input pulse was not a Fourier-transform-limited one (see Ref. [22] for more details). For the ACFs shown in Fig. 4b, the pulse compression factor *F* was ~4.7. Note that the CafCA method cannot degrade the long-range contrast of the pulse, since the transmission of the pulse wings through the plates is linear, and the dispersion of the plates and CMs is insufficient for the appearance of pre-pulses or post-pulses far from the main pulse.

The CafCA method is efficient for laser beams with a uniform intensity distribution in the near field, since for practical use, in addition to the factor of pulse compression, the radia-

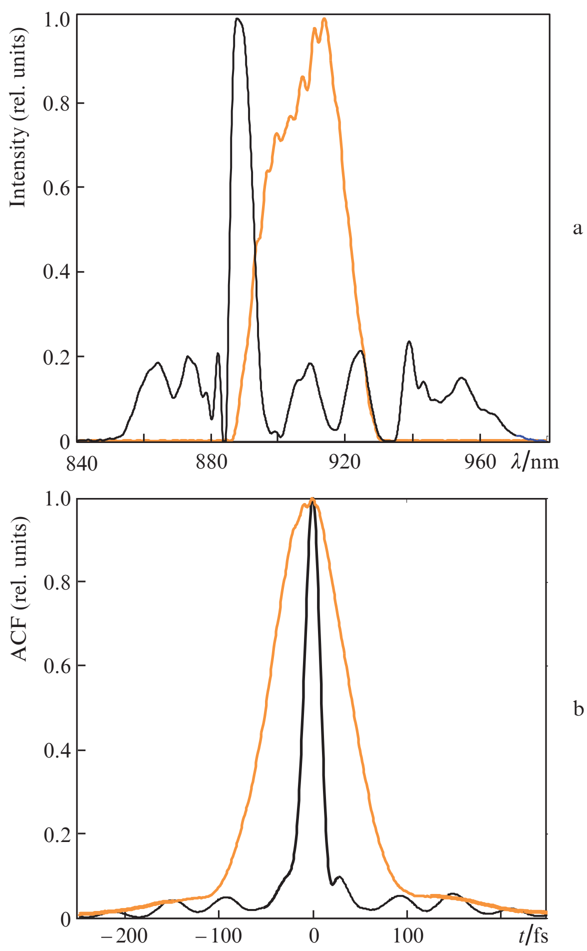


**Figure 4.** (a) Spectra and (b) ACF of the input (grey curves) and output (black curves) pulses.

tion quality in the far-field zone is of key importance. The nonuniformity of the beam intensity distribution leads to nonuniformity of the transverse spatial phase and deteriorates the focusing, which, however, can be compensated by adaptive optics. An experimental study of this issue is beyond the scope of this paper; theoretical estimates can be found in Refs [10, 13]. Note that with optimal compression, the power increase factor at one stage is 1 + *B*/2 [22] and, therefore, when the power increase factors are equal, the two-stage scheme requires a smaller total *B*-integral, so that the spatial phase distortions in it will be smaller than in a single-stage scheme.

Despite the large values of the *B*-integral (up to 8 at the first stage and the same order in the second one), small-scale self-focusing was suppressed due to self-filtering. There were no damages on the plates or on the CMs. In addition, when removing and introducing the plates into the beam, we did not find any significant changes in the beam intensity distribution in the near field, which also indicates the absence of small-scale self-focusing.

Note that in two-stage geometry, suppression of small-scale self-focusing is much more efficient than in single-stage geometry, not only because self-filtering is performed twice, but also because the intensity and duration of the pulse in nonlinear plates of the first and second stages are significantly different: the intensity increases and the duration decreases. Due to the significantly higher intensity, the maxima of the increment of self-focusing instability occur at significantly different transverse wave numbers, which reduces the total noise gain [13]. According to theoretical predictions [23, 24], a shorter pulse facilitates additional suppression of small-scale self-focusing due to nonlinear dispersion (the dependence of group velocity on intensity).

## 3. Conclusions

Two-stage nonlinear compression of femtosecond laser pulses (nonlinear element, CM, another nonlinear element and another CM, see Fig. 1) was earlier used only at the micro-joule energy level. We demonstrated the possibility of such an approach for compressing femtosecond laser pulses with an energy of 17 J and a power of more than 200 TW. The key point for such significant scaling is the suppression of small-scale self-focusing due to self-filtering of the laser beam during its propagation in free space. Due to using this technique, no traces of self-focusing were detected, although the value of the $B$-integral reached eight at the first stage and was approximately the same at the second one. A five-fold compression of the pulse was demonstrated, and the duration of the output pulse was limited by the parameters of chirping mirrors available in the experiment. Note that this simple and cheap method of repeatedly increasing the pulse power has an almost 100% energy efficiency and can be used at the output of any ultrahigh-power lasers.

## References


1. Fisher R.A., Kelley P.L., Gustajson T.K. *Appl. Phys. Lett*., **14**, 140 (1969).
2. Laubereau A. *Phys. Lett*., **29A**, 539 (1969).
3. Shank C.V., Fork R.L., Yen R., Stolen R.H., Tomlinson W.J. *Appl. Phys. Lett*., **40**, 761 (1982).
4. Nisoli M., Silvestri S.D., Svelto O. *Appl. Phys. Lett*., **68**, 2793 (1996).
5. Lavenu L., Natile M., Guichard F., Zaouter Y., Delen X., Hanna M., Mottay E., Georges P. *Opt. Lett*., **43**, 2252 (2018).
6. Rolland C., Corkum P.B. *J. Opt. Soc. Am. B*, **5**, 641 (1988).
7. Mironov S.Yu., Ginzburg V.N., Yakovlev I.V., Kochetkov A.A., Shaykin A.A., Khazanov E.A., Mourou G. *Quantum Electron*., **47**, 614 (2017) [*Kvantovaya Elektron*., **47**, 614 (2017)].
8. Farinella D.M., Wheeler J., Hussein A.E., Nees J., Stanfield M., Beier N., Ma Y., Cojocaru G., Ungureanu R., Pittman M., Demailly J., Baynard E., Fabbri R., et al. *J. Opt. Soc. Am. B*, **36**, A28 (2019).
9. Ginzburg V.N., Yakovlev I.V., Zuev A.S., Korobeynikova A.P., Kochetkov A.A., Kuzmin A.A., Mironov S.Yu., Shaykin A.A., Shaikin I.A., Khazanov E.A. *Quantum Electron*., **49**, 299 (2019) [*Kvantovaya Elektron*., **49**, 299 (2019)].
10. Ginzburg V., Yakovlev I., Zuev A., Korobeynikova A., Kochetkov A., Kuzmin A., Mironov S., Shaykin A., Shaikin I., Khazanov E., Mourou G. *Phys. Rev. A*, **101**, 013829 (2020).
11. Mironov S.Y., Lozhkarev V.V., Ginzburg V.N., Yakovlev I.V., Luchinin G., Shaykin A.A., Khazanov E.A., Babin A.A., Novikov E., Fadeev S., Sergeev A.M., Mourou G.A. *IEEE J. Sel. Top. Quantum Electron*., **18**, 7 (2010).
12. Mironov S., Lozhkarev V., Luchinin G., Shaykin A., Khazanov E. *Appl. Phys. B*, **113**, 147 (2013).
13. Khazanov E.A., Mironov S.Yu., Mourou G. *Phys. Usp*., **62**, 1096 (2019) [*Usp. Fiz. Nauk*, **189**, 1173 (2019)].
14. Seidel M., Brons J., Arisholm G., Fritsch K., Pervak V., Pronin O. *Sci. Rep*., **7**, 1410 (2017).
15. Seidel M., Arisholm G., Brons J., Pervak V., Pronin O. *Opt. Express*, **24**, 9412 (2016).
16. Nikolaus B., Grischkowsky D. *Appl. Phys. Lett*., **43**, 228 (1983).
17. Vysotina N.V., Rozanov N.N., Yashin V.E. *Opt. Spectrosc*., **110** (6), 973 (2011) [*Opt. Spektrosk*., **110**, (6) 1029 (2011)].
18. Voronin A.A., Zheltikov A.M., Ditmire T., Rus B., Korn G. *Opt. Commun*., **291**, 299 (2013).
19. Mourou G., Mironov S., Khazanov E., Sergeev A. *Eur. Phys. J. Spec. Top*., **223**, 1181 (2014).
20. Lozhkarev V.V., Freidman G.I., Ginzburg V.N., Katin E.V., Khazanov E.A., Kirsanov A.V., Luchinin G.A., Mal'shakov A.N., Martyanov M.A., Palashov O.V., Poteomkin A.K., Sergeev A.M., Shaykin A.A., Yakovlev I.V. *Laser Phys. Lett*., **4**, 421 (2007).
21. Ginzburg V.N., Kochetkov A.A., Mironov S.Yu., Potemkin A.K., Silin D.E., Khazanov E.A. *Izv. Vyssh. Uchebn. Zaved., Ser. Radiofiz*., **62** (2019) (to be published).
22. Ginzburg V.N., Kochetkov A.A., Yakovlev I.V., Mironov S.Yu., Shaykin A.A., Khazanov E.A. *Quantum Electron*., **46**, 106 (2016) [*Kvantovaya Elektron*., **46**, 106 (2016)].
23. Balakin A.A., Litvak A.G., Mironov V.A., Skobelev S.A. *J. Optics*, **19**, 095503 (2017).
24. Balakin A.A., Kim A.V., Litvak A.G., Mironov V.A., Skobelev S.A. *Phys. Rev*., **94**, 043812 (2016).